Journal of the Korean Physical Society, Vol. 70, No. 12, June 2017, pp. 1077∼1082

Verification of SuperMC for Simulation of a High-Dose-Rate Brachytherapy Source

Hamza Naeem and Muhammad Abdul Wasaye
Key Laboratory of Neutronics and Radiation Safety, Institute of Nuclear Energy Safety Technology, Chinese Academy of Sciences, Hefei, Anhui, 230031, China; Collaborative Innovation Center of Radiation Medicine of Jiangsu Higher Education Institutions, Suzhou 215006, China; and University of Science and Technology of China, Hefei, Anhui, 230027, China

Chaobin Chen, Huaqing Zheng and Lijuan Hao*
Key Laboratory of Neutronics and Radiation Safety, Institute of Nuclear Energy Safety Technology, Chinese Academy of Sciences, Hefei, Anhui, 230031, China; and Collaborative Innovation Center of Radiation Medicine of Jiangsu Higher Education Institutions, Suzhou 215006, China

(Received 17 April 2017)

In this study, SuperMC (Super Monte Carlo simulation program for nuclear and radiation simulation) was tested and verified for simulation of a high-dose-rate brachytherapy source. The Monte Carlo simulation includes calculations of the air kerma strength, dose rate constant, radial dose function and anisotropy function as recommended by the American Association of Physicists in Medicine (AAPM) in Task Group reports 43 and 43U1 (TG-43, TG-43U1). The air kerma strength, dose rate constant, radial dose function and anisotropy function were compared with previously published Monte Carlo simulation results and experimental data. The calculated parameters were found to be in good agreement with published Monte Carlo and measured data. The value obtained from the SuperMC simulation for the air kerma strength was 9.779×10^{-8} U·Bq^{-1} and the dose rate constant was $1.1092 \pm 0.02\%$ cGy·h^{-1}·U^{-1}. The time to transport 5×10^7 photons showed SuperMC to be relatively faster than MCNP. The results show that SuperMC can be used for fast and accurate simulations and dosimetric calculations of HDR brachytherapy sources.

PACS numbers: 87.10.Rt
Keywords: Monte Carlo, SuperMC, ^{192}Ir, High dose rate, TG-43, Brachytherapy
DOI: 10.3938/jkps.70.1077

I. INTRODUCTION

Brachytherapy is a method of radiotherapy in which sealed radionuclides are placed near the surface to be treated so that the source to surface distance (SSD) is comparable to the treatment depth, resulting in a rapid dose fall off. This is achieved by (i) placing the source directly onto the surface to be treated (molds, plaques, beta applicators), (ii) inserting the sources into body cavities (intra-cavity), and (iii) implanting the source, temporarily or permanently, directly into the tumor (interstitial).

^{192}Ir high dose rate (HDR) brachytherapy sources are usually used for the treatment of cervix, breast, prostate, lungs *etc.* tumors [1]. Clinically theses sources require an accurate determination of all the dosimetric parameters, that are necessary for the treatment planning system (TPS) [2]. The American Association of Physicists in Medicine (AAPM) has recommended in task group reports 43 and 43U1 (TG-43, TG-43U1) [3,4] that as inputs for the TPS, accurate dosimetric data on a realistic geometry and on the mechanical characteristics of the sources must be acquired using standard methods.

Experimental dosimetry in brachytherapy is very complex because of the high dose abruptness near the source and is even impossible at very small distances. Also, the dose fluctuation with solid angle in a 4Pi geometry of the source should be analyzed because ordinary experimental measurements do not represent this. One of the most widely used technique to solve this issue is a Monte Carlo (MC) simulation of transport. In modern brachytherapy, a MC simulation is the primary dosimetry tool and plays a key role in clinical practice and research. The most recognized application of MC methods in brachytherapy is the determination of the dose distributions around individual radiation sources [5]. Prior

*E-mail: lijuan.hao@fds.org.cn

to the calculation of the dosimetric parameters through MC methods, a validation of the Monte Carlo transport code for brachytherapy must be done using experimental data and other Monte Carlo codes that have already been validated extensively, such as EGSnrc [6], MCNP [7], PENELOPE [8].

In this study, the SuperMC code was tested by calculating the air kerma strength, dose rate constant, radial dose function, and anisotropy function of the ^{192}Ir microselectron v2 HDR brachytherapy source according to the AAPM TG-43 and TG-43U1 formalisms. The verification was done by comparing the dosimetric parameters obtained in this study with those obtained in other Monte Carlo studies such as those of Taylor and Rogers [6] using EGSnrc code simulations, Daskalov *et al.* [9] using MCPT code simulations, and Lopez *et al.* [8] using PENELOPE code simulations. Further simulation results were compared with the measurements of Sharma *et al.* [10]. The MCNP was also used to verify the dosimetric results calculated through SuperMC.

II. MATERIALS AND METHODS

1. Super Monte Carlo (SuperMC) Code Description

SuperMC is a CAD-based general purpose Monte Carlo program and is currently under development by the FDS (Fusion Driven System) Team in China [11]. SuperMC is designed for high-fidelity simulations of radiation sources and detectors, medical physics analyses, safety analysis of nuclear systems, *etc.* It is also designed to be coupled with deterministic transport methods. The latest released version of SuperMC is equipped with the functions of automatic modeling, visualization, simulation and cloud computing. SuperMC has been applied to the studies of the FDS-I [12,13], FDS-II [14,15], FDS-III [16], FDS-ST [17, 18], ITER [19, 20] fusion reactors and other reactor [21–23] and is designed for the Monte-Carlo-based dose-calculation engine of KylinRay (Accurate Radiotherapy System) [24,25].

In SuperMC, CAD models can be automatically converted to MC calculation geometry models. The geometry models are represented by Constructive Solid Geometry (CSG), which is based on primitive solids. Advance geometry acceleration methods, such as the neighbor search method, axis-aligned bounding box method and 3D spatial subdivision method, have been designed to improve the efficiency of geometry navigation in the simulation [11]. Besides the CAD geometry, CT images can be converted to geometry models for dose calculations in radiation shielding or medical physics [26].

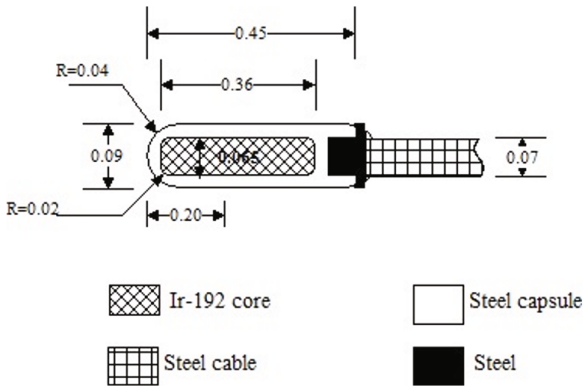

Fig. 1. MicroSelectron-HDR ^{192}Ir source design used in this work. Dimensions are in cm.

2. Radioactive Source Description

Figure 1 illustrates the details of the geometry design and the material composition of the microSelectron v2 HDR ^{192}Ir source used in our SuperMC calculations. The active core is a pure ^{192}Ir metal cylinder and has a length of 3.6 mm and a diameter of 0.65 mm. Uniform exposure is expected to be distributed around it. The core is encapsulated in stainless steel (SS) having a 4.5-mm length and a 0.9-mm outer diameter and woven steel cable having a 0.7-mm diameter. The capsule and the cable are made of steel but with different densities. The densities of the Ir metal, the stainless steel (SS), and the woven steel cable are 22.39, 8.02, and 4.81 g/cm^3 respectively.

The half-life of ^{192}Ir is 73.825 days [27], and one average decay will emit one electron and 2.363 photons. The source activity, A, as a function of the number of photons released per sec, N_{photon}, can be expressed as

$$N_{photon} = A \cdot (2.363 \pm 0.3\%) \quad [\text{photon} \times \text{s}^{-1}], \quad (1)$$

where the uncertainty is calculated from the published spectrum of ^{192}Ir by Duchemin and Coursol [27].

3. TG-43 Dose Calculation Formalism

The AAPM TG-43 dose calculation formalism is designed to calculate the dose at any specific point (r, θ) relative to the source's center. All quantities are designed to be evaluated using sparse dose-rate grids, which are derived from measurements or Monte Carlo calculations. The dose rate, $D(r, \theta)$, at (r, θ) is calculated in the TG-43 model by using

$$\dot{D}(r, \theta) = S_k \times \Lambda \times \frac{G(r, \theta)}{G(r_0, \theta_0)} \times g(r) \times F(r, \theta), \quad (2)$$

where S_k is the air kerma strength, Λ is the dose rate constant, $G(r, \theta)$ is the geometry function, $g(r)$ is the radial dose function and $F(r, \theta)$ is the anisotropy function.

The brachytherapy source strength can be determined by using the air kerma strength, S_k in terms of U, can be written as

$$S_k = \dot{K}_{air}(d) \times d^2, \tag{3}$$

where $\dot{K}_{air}(d)$ is the air kerma rate in free space at a specified distance, d. The dose rate constant, Λ, is the ratio of the dose rate at a reference position to S_k and can be written as follows

$$\Lambda = \frac{\dot{D}(r_0, \theta_0)}{S_k}. \tag{4}$$

The radial dose function, $g_L(r)$, is a relative dose function that accounts for the variation of the dose with perpendicular distance from the source due to photon attenuation or absorption and can be written as (using the line-source approximation)

$$g_L(r) = \frac{\dot{D}(r, \theta_0)}{\dot{D}(r_0, \theta_0)} \times \frac{\dot{G}(r_0, \theta_0)}{\dot{G}(r, \theta_0)}. \tag{5}$$

The anisotropy function, $F(r, \theta)$, is the dose variation as a function of the polar angle at a given distance around the source and can be written as

$$F(r, \theta) = \frac{\dot{D}(r, \theta)}{\dot{D}(r, \theta_0)} \times \frac{\dot{G}(r, \theta_0)}{\dot{G}(r, \theta)}. \tag{6}$$

4. Monte Carlo Simulations

In this study, the air kerma strength and the dose distribution of ^{192}Ir brachytherapy source were simulated using the SuperMC v3.0 Monte Carlo code developed by the FDS team in China [11]. MCNP5, a particle transport code developed by Los Alamos National Laboratory [28], has been extensively used for dosimetric calculations in different areas of medical physics, such as brachytherapy, radiotherapy, radiation protection *etc.* [29]. Therefore, to validate SuperMC for dosimetric calculations involving brachytherapy sources, we also did Monte Carlo calculations of these dosimetric parameters by using MCNP5. For both SuperMC and MCNP5, ^{192}Ir source spectrum was obtained from Duchemin and Coursol [27] and the photon cross-section was taken from ENDF/B-VII [30]. The photon cut off was set to be 1 keV. Dose calculations were carried out with the source placed at the center of a spherical water phantom (density: $\rho = 0.998$ g/cm^3) with a radius of 30 cm. Some dose calculations were carried out in a spherical water phantom with a radius of 15 cm to make a comparison with the data published by Daskalov *et al.* [9]. The time to transport 5×10^7 photons was recorded for both SuperMC and MCNP by using a single core running at window 7. The water phantom and the ^{192}Ir source were modeled by using the automatic and intelligent CAD-based modeling module of SuperMC. This modeling function of SuperMC significantly reduces the manpower and enhances the reliability of the calculation model. More features of SuperMC/MCAM are discussed elsewhere [9].

The air kerma strength per unit source activity S_k/A, in terms of UBq^{-1}, was calculated by placing a small sphere of dry air with a volume of 0.05 cm^3 at a distance, d, of 100 cm in a direction perpendicular to the axis of the source. The source was placed at the center of a spherical *vacuum* phantom with a radius 100 cm. The air kerma per initial particle is given by

$$\frac{S_k}{A} = 3.6 \times 10^9 \times 1.602 \times 10^{-10} \times 2.363 \times \sum_{5\ \text{keV}}^{E_{max}} \Phi(E_i) \times \left(\frac{\mu_{en}(E_i)}{\rho}\right) \times \Delta E \qquad [\text{UBq}^{-1}] \tag{7}$$

where E_i and ΔE are the central point of each energy bin and the energy bin size respectively. $\left(\frac{\mu_{en}(E_i)}{\rho}\right)$ is the X-ray mass energy-absorption coefficient for air at energy E_i taken from the NIST compilation by interpolation [31]. $\Phi(E_i)$ [MeV^{-1}cm^{-2}] is the photon fluence differential in energy within each energy bin. The factor 1.602×10^{-10} is necessary to convert $\dot{K}_{air}$ from MeVg^{-1} to Gy while the factor 2.363 is taken from Eq. (1). The factor 3.6×10^9 is used to convert the unit Gym^{2}s^{-1}Bq^{-1} to UBq^{-1}.

The radial dose distributions were calculated in 0.5-cm radial increments up to 14 cm while the anisotropic dose distributions were setup for 5° increments from 0° to 180° from the axis through the center of the device along the woven cable. To estimate $\dot{K}_{air}$ and calculate the absorbed dose to water at each radial distance and angular distribution, we used the energy deposition tally (T6) in SuperMC.

III. RESULTS AND DISCUSSION

The results for the air kerma strength per unit source activity and the dose rate constant at their reference position are presented in Table 1 and are compared with their respective published experimental and Monte Carlo

Table 1. Comparison of and from this study with those from published Monte Carlo and experimental studies.

	This Work		Published Monte Carlo Studies			Experimental Studies
S_k/A (U·Bq^{-1})	SuperMC	MCNP	Borg and Rogers using EGSnrc [31]	Daskalov *et al.* using MCPT [9]	Lopez *et al.* using PENELOPE [8]	Anctil *et al.* [32]
	9.779×10^8	9.776×10^8	9.71×10^8	-	9.78×10^8	-
Λ (cGy·h^{-1}·U^{-1})	1.1092 ± 0.02%	1.109 ± 0.02%	1.1092 ± 0.02%	1.1092 ± 0.11%	1.1119 ± 0.04%	1.134 ± 2.9%

Table 2. Computational time comparison to simulate primary photons from a ^{192}Ir source in a water phantom with different numbers of volume elements.

number of volume elements	Time (min)	
	SuperMC	MCNP
7×10^3	39.64	40.03
8×10^4	64.07	65.93
2.5×10^5	70.60	78.92
2×10^6	110.23	133.54

simulated results. The air kerma strength per unit source activity is estimated from the Monte Carlo calculated photon fluence spectrum around the source. These estimates do not include the bremsstrahlung contribution to the air kerma strength. A comparison of S_k/A and Λ shows that the values obtained in this simulation agree well with the previously published values. We note that the uncertainties in the above comparison are statistical uncertainties.

Table 2 shows a computational-time comparison between SuperMC and MCNP to simulate 5×10^7 primary photons as a function of the number of volume elements (or voxels). It has been observed that SuperMC and MCNP have simulated 10^4 volume elements in approximately 65 minutes while for a maximum number of elements, SuperMC is approximately 1.2 times faster than MCNP.

The radial dose function $g_L(r)$ was determined by using the line source approximation at 18 different radial distances ranging from 0.5 to 20 cm along the transverse axis as shown in Fig. 2. Also, $g_L(r)$ was determined at 14 different radial distances from 0.5 to 14 cm. A comparison between the simulated results of this work and previous results shows that, at $0.5 \leq r \leq 20$ cm, our values are 0.5% (on average) less than the values calculated by Taylor and Rogers [6] and Lopez *et al.* [8] while at $0.5 \leq r \leq 14$ cm, our values are 0.2% (on average) greater than the values calculated by Daskalov *et al.* [9]. The radial dose function is observed to depend on the phantom size, as the differences are less than 0.2% up to a radius of 5 cm and increase rapidly with increasing

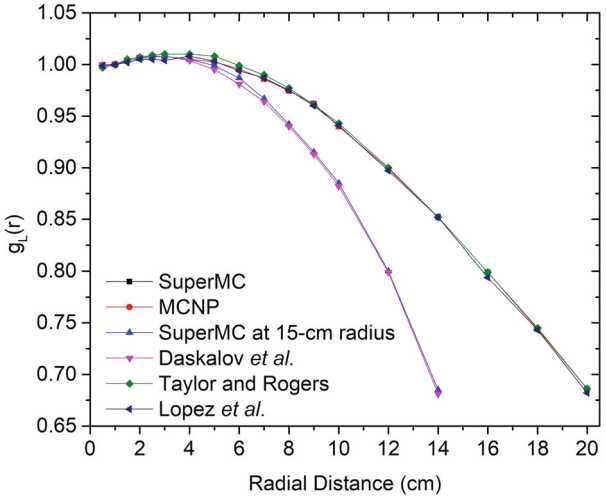

Fig. 2. (Color online) Radial dose function calculated in a spherical phantom with a radius of 30 cm.

radius thereafter.

The values of the anisotropy function $F(r, \theta)$ at 1.0, 2.0, and 5.0 cm for angles 0° to 180° are presented in Fig. 3. Figures 3(a) - (c) show a comparison of the anisotropy function obtained in this work with published experimental data and Monte Carlo studies. The difference between the values of the anisotropy function at each radial position is less than 2%. Anisotropy function has been observed not to depend on the phantom size.

With the automatic modeling of SuperMC, the user can define the actual geometry of the source model, which not only reduce the manpower but also increase the efficiency. Results show that the modeling function of SuperMC is accurate and that the transport algorithm is generic. Furthermore, it can be used in brachytherapy applications, *e.g.* for accurate modeling of applicators, *etc.*.

IV. CONCLUSION

In this study, validation and verifications methods as recommended by AAPM TG43, were adopted to validate the performance of SuperMC for a ^{192}Ir microSe-

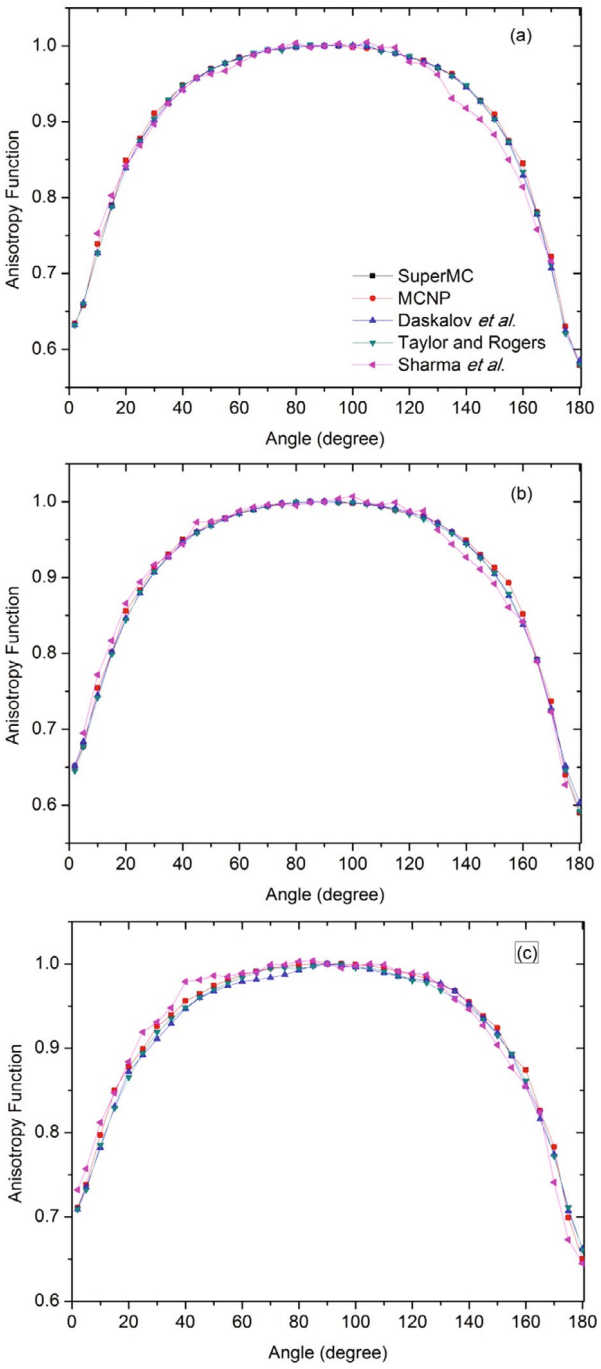

Fig. 3. (Color online) Anisotropy function calculated in a spherical phantom with a radius of 30 cm at radii of (a) 1.0 cm, (b) 2.0 cm, and (c) 5.0 cm.

lectron v2 HDR brachytherapy source. The air kerma strength, dose distribution (in water), radial dose function and anisotropy function were calculated to test SuperMC. Our results were compared with the experimental data set of Sharma *et al.* [10] and the Monte Carlo studies of Daskalov *et al.* [9], Taylor and Rogers [6] and Lopez *et al.* [8]. The results obtained with SuperMC were in very good agreement with the results from other published Monte Carlo and experimental studies. SuperMC is concluded to be relatively faster than MCNP and can be used for accurate modeling, simulation and calculation of high-dose-rate brachytherapy sources.

ACKNOWLEDGMENTS

This work was supported by the National Natural Science Foundation of China (No. 11605233No. 11305205, No. 11305203 and No. 11405204), the National Natural Science Foundation of Anhui Provincial (No. 1308085QH138 and No. 1508085QH180), Anhui Provincial Special Project for High Technology Industry and Special Project of Youth Innovation Promotion Association of the Chinese Academy of Sciences, and the Industrialization Fund. In addition, the authors would like to thank the great help from other members of the FDS Team.

REFERENCES

[1] Alain Gerbaulet, Richard Pötter, Jean-Jacques Mazeron, Harm Meertens and Erik Van Limbergen, ESTRO (2002).
[2] R. Nath, L. L. Anderson, J. A Meli, A. J. Olch, J. A. Stitt and J. F. Williamson, Med. Phys. **24**, 1557 (1997).
[3] R. Nath, L. L. Anderson, G. Luxton, K. A. Weaver, J. F. Williamson and A. S. Meigooni, Med. Phys. **22**, 209 (1995).
[4] M. J. Rivard, B. M. Coursey, L. A. DeWerd, W. F. Hanson, M. S. Huq, G. S. Ibbott, M. G. Mitch, R. Nath and J. F. Williamson, Med. Phys. **31**, 633 (2004).
[5] B. R. Thomadsen, M. J. Rivard, W. M. Butler and L. Beach, Med. Phys. **33**, 1185 (2006).
[6] R. E. P. Taylor and D. W. O. Rogers, Med. Phys. **35**, 4933 (2008).
[7] G. P. Fonseca, R. A. Rubo, R. A. Minamisawa, G. R. dos Santos, P. C. G. Antunes and H. Yoriyaz, Med. Phys. **40**, 051717 (2013).
[8] J. F. A. López, J. T. Donaire and R. G. Alcalde, Rev. Fis. Med. **12**, 159 (2011).
[9] G. M. Daskalov, E. Loffler and J. F. Williamson, Med. Phys. **25**, 2200 (1998).
[10] S. D. Sharma, C. Bianchi, L. Conte, R. Novario and B. C. Bhatt, Phys. Med. Biol. **49**, 4065 (2004).
[11] Y. Wu, J. Song, H. Zheng, G. Sun, L. Hao, P. Long and L. Hu, Ann. Nucl. Energy **82**, 161 (2015).
[12] Y. Wu, J. Jiang, M. Wang and M. Jin, Nucl. Fusion **51**, 103036 (2011).
[13] Y. Wu, S. Zheng, X. Zhu, W. Wang *et al.*, Fusion Eng. Des. **81**, 1305 (2006).
[14] Y. Wu, Fusion Eng. Des. **83**, 1683 (2008).
[15] Y. Wu, Fusion Eng. Des. **81**, 2713 (2006).
[16] Y. Wu, J. Nucl. Mater. **386-388**, 122 (2009).
[17] L. Qiu, Y. Wu, B. Xiao, Q. Xu, Q. Huang, B. Wu, Y. Chen, W. Xu, Y. Chen and X. Liu, Nucl. Fusion **40**, 629 (2000).

[18] Y. X. Chen and Y. C. Wu, Fusion Eng. Des. **49-50**, 507 (2000).
[19] Y. Wu, Nucl. Fusion **47**, 1533 (2007).
[20] Y. Wu, Fusion Eng. Des. **82**, 1893 (2007).
[21] Y. Wu, Fusion Eng. Des. **63-64**, 73 (2002).
[22] Y. Wu, L. Qiu and Y. Chen, Fusion Eng. Des. **51-52**, 395 (2000).
[23] Q. Huang, J. Li and Y. Chen, J. Nucl. Mater. **329**, 268 (2004).
[24] W. U. Yi-can and C. A. O. Rui-fen, Chinese Phys. C **32**, 177 (2008).
[25] R. Cao, Y. Wu, X. Pei, J. Jing, G. Li, M. Cheng, G. Li and L. Hu, Chinese Phys. C **35**, 313 (2011).
[26] M. Cheng, Q. Zeng, R. Cao, G. Li and H. Zheng, Prog. Nucl. Sci. Technol. **2**, 237 (2011).
[27] B. Duchemin and N.Coursol. DAMRI/LMRI, CEA, France (1990).
[28] M. A. General and M. Carlo, LA-UR-03-1987 X-5 Monte Carlo Team, 836 (2003).
[29] D. Granero, J. Vijande, F. Ballester and M. J. Rivard, Med. Phys. **38**, 487 (2011).
[30] M. B. Chadwick, P. Obložinský, M. Herman, N. M. Greene *et al.*, Nucl. Data Sheets **107**, 2931 (2006).
[31] J. Borg and D. W. O. Rogers, *Monte Carlo Calculations of Photon Spectra in Air from* ^{192}*Ir Sources* (National Research Council, Canada, 1999).
[32] J. C. Anctil, B. G. Clark and C. J. Arsenault, Med. Phys. **25**, 2279 (1998).